WORLD CONFERENCE ON TIMBER ENGINEERING 2025
BRISBANE, AUSTRALIA
Advancing Timber for the Future Built Environment

SHEAR PERFORMANCE INVESTIGATION ON THE NOTCH-SCREW CONNECTIONS FOR TIMBER-UHPC COMPOSITE STRUCTURES

Xiaoyue Zhang [1]*, Wanru Huang [2], Jiajia Ou [3], Fengjiang Qin [4], Weiguo Long [5], Di Chen [6]

ABSTRACT: This paper presents the shear behavior of notch-screw shear connectors used in glulam-UHPC composite (GUCC) structures. Seven groups of push-out specimens with different notch length, notch depth and the shear length in front of the notch were prepared and tested in direct shear under monotonic loading conditions. The experimental determination of the strength, the slip modulus and the failure modes were made by push-out tests. Subsequently, a numerical modelling using ABAQUS was carried out in order to develop a three-dimensional numerical model that represented the connection. The results indicated that direct UHPC shear failure was the main failure mode for the notched connections. The notch length and notch depth significantly influenced the load-carrying capacity and slip stiffness of the specimens combining a notch and two screws. Comparing numerical and experimental results demonstrated that the numerical model could accurately predict the failure load and the slip modulus of the connection.

KEYWORDS: Timber-UHPC composite structure, Notch-screw connectors, Push-out tests, Finite element modeling

1 – INTRODUCTION

1.1 BACKGROUND

Timber-concrete composite (TCC) structures optimize multiple performances, including structural stiffness, lightness, vibration comfort and energy conservation. They have been widely used in the construction of buildings and small-span bridges [1]. However, traditional TCC beams still face several issues in practical applications, such as the heavy thickness of conventional concrete deck panels. These factors reduce the overall load-bearing performance and durability of the composite beam.

1.2 GUCC STRUCTURE

A new glulam-UHPC composite (GUCC) structure was proposed to address this issue, featuring a thinner deck to decrease the weight and significantly reduce long-term deflection due to the minimal creep deformation of UHPC. The GUCC structure fully utilizes the high tensile strength of glulam parallel to grain and the high compressive strength of UHPC, demonstrating promising application prospects in both building and bridge structures. For composite beams composed of two different materials, reliable connectors are crucial to ensure efficient combination. Therefore, investigating their mechanical properties, shear-resistance mechanisms, and failure modes is of paramount importance. Studies have shown that the notched connection offer significant advantages in terms of shear strength and slip modulus compared to screwed-type connections [2]. The structural behaviour and failure modes of composite systems are strongly influenced by the geometry of notched connections and the material properties of timber and concrete. Therefore, further research on the geometry of the notch connection is necessary. A schematic of the notch-screw connector as shown in Figure 1.

1.3 OBJECTIVE

The objective of this research was to investigate the shear behaviour of notch+screw connectors in GUCC structures made of glulam girder and UHPC slab. A combined approach of push-out tests and nonlinear finite element simulation to explore the influence of different design parameters on the shear performance of notch+screw connectors.

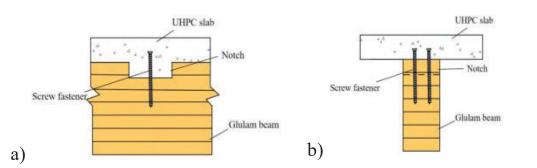

Figure 1. A schematic of the notch-screw connector: a) Longitudinal cross-section of the composite beam; b) Transverse cross-section of the composite beam.

[1] Xiaoyue Zhang, Chongqing University, Chongqing, China, xiaoyuezhang@cqu.edu.cn
[2] Wanru Huang, Chongqing University, Chongqing, China, 13364030956@163.com
[3] Jiajia Ou, China Southwest Architectural Design and Research Institute Corp. Ltd., Chengdu, China, ouyangjia28@126.com
[4] Fengjiang Qin, Chongqing University, Chongqing, China, qinfengjiang@cqu.edu.cn
[5] Weiguo Long, China Southwest Architectural Design and Research Institute Corp. Ltd., Chengdu, China, xnymjg@cscec.com
[6] Di Chen, China Southwest Architectural Design and Research Institute Corp. Ltd., Chengdu, China, sechendi@outlook.com

https://doi.org/10.52202/080513-0137

Table 3: Dimension parameters of specimens

Series		Notch (mm)				Number of screws	Number of replicates
		l_n	d_n	w_n	l_v		
S1	SA-70-20-400-2	70	20	135	400	2	2
S2	SA-70-35-400-2	70	35	135	400	2	2
S3	SA-70-50-400-2	70	50	135	400	2	2
S4	SA-110-50-400-2	110	50	135	400	2	2
S5	SA-150-50-400-2	150	50	135	400	2	2
S6	SA-70-50-200-2	70	50	135	200	2	2
S7	SA-70-50-600-2	70	50	135	600	2	2

2 – EXPERIMENTAL INVESTIGATIONS

2.1 MATERIALS

In this study, Douglas fir GLT (classified as TCT36) was used as the glulam material. The thickness of each layer of the laminated timber in the GLT is 35 mm, and the adhesive used is melamine formaldehyde. According to BS EN 13183-1:2002 [3], the physical density and moisture content of the glued laminated timber are 505.34 kg/m³ and 11.63%, respectively. To evaluate the compressive strength and elastic modulus of the timber parallel to the grain, tests were conducted following the guidelines of EN 408 [4]. For these tests, prismatic specimens of 20 mm × 20 mm × 30 mm were used to determine compressive strength, and 20 mm × 20 mm × 60 mm specimens were used to assess the Young's modulus. Additionally, shear strength was measured using specimens of 40 mm × 35 mm × 20mm, in accordance with ASTM D905 [5].

The UHPC used in this experiment was produced by Jiangsu Sobute New Materials Co., Ltd., with the model designated as UDC(II)-15. The steel fibers utilized were straight copper-coated fibers with a diameter of 0.2 mm and a length of 12.7 mm, with a volumetric content of approximately 2%. The mechanical properties of UHPC were determined in accordance with the T CBMF 37-2018 [6]. The mechanical properties of the glulam and UHPC derived from these tests are systematically presented in Table 1 and Table 2.

Table 1: Mechanical properties of glulam (MPa)

Component	$f_{t,c}$	E_t	$f_{t,s}$	$f_{t,b}$
Glulam	51.87	12608.16	6.32	53.51

Table 2: Mechanical properties of UHPC (MPa)

Component	$f_{c,c}$	E_c	$f_{c,t}$
UHPC	126	42630	7.1

2.2 TEST DESIGN

A total of seven different configurations of notched connections were designed, with each configuration had two repetitions. Each group combined 135 mm wide rectangle notches with two STSs. Figure 2 displays the dimension of the glulam and UHPC slab, considering key factors such as the shear length of the glulam, the length of the notches, the depth of the notches. The notch length varied between 70mm and 150mm (70, 110, and 150mm). The shear length of the glulam varied from 200 mm to 600 mm (200, 400 and 600mm). The depth of the notch varied between 20 mm and 50 mm (20, 35 and 50mm). The dimension parameters of specimens are shown in Table 3.

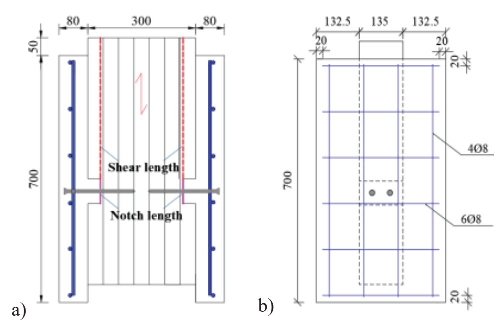

Figure 2. Specimen design: a) front view; b) side view

2.3 TEST SETUP

The loading device for the push-out specimens is shown in Figure 3. Four Linear Variable Differential Transformers (LVDTs) (labelled L_1, L_2, L_3 and L_4) were symmetrically arranged at the front, rear, left, and right positions of each specimen to measure the relative slip at the interface between the glulam beam and the UHPC slabs. To prevent lateral movement of the UHPC slab's bottom during loading, angle steel and bolt rods were used to provide appropriate constraints at both the top and bottom of the specimens. During the loading process,

https://doi.org/10.52202/080513-0137

a force sensor F_1 installed at the top of the specimen was used to measure the applied force.

The push-out test was conducted using a universal testing machine (1000kN) and loading protocol according to the European standard EN26891:1991 [7], as shown in Figure 4a). Before using this loading protocol, it was necessary to estimate the shear bearing capacity of each set of connections. The estimated shear bearing capacity can be determined by referring to literature or previous research. Assuming that the estimated shear-bearing capacity of the connection was denoted as F_{est}, the loading process was conducted as follows: First, load control was applied, and the load was increased to 0.4 F_{est} at a rate of 0.2 F_{est}/min, maintaining this load level for 30 seconds; Subsequently, the load was reduced to 0.1 F_{est} the same loading rate and held at this level for 30 seconds; Then, the load was increased again to 0.7 F_{est} at the same rate. Finally, the loading mode was switched to displacement control, applying a displacement rate of 2 mm/min until the failure of the connections. The typical load-slip relationship of the connections obtained using the loading protocol shown in Figure 4b).

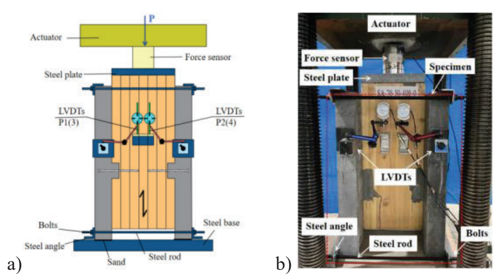

Figure 3. Test set-up: a) schematic; b) physical diagram.

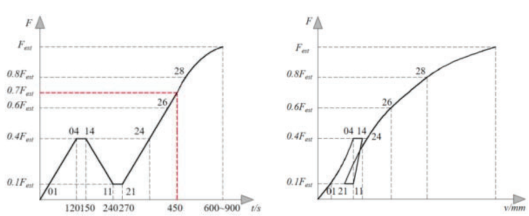

Figure 4. Loading protocol and ideal loads-slip curve[7]: a) loading procedure; b) ideal load-slip curve

The determination of the slip modulus for the specimens across various stress stages was conducted following standard EN 26,891 [7]. In this study, the modulus is defined as the secant slip modulus of the 40% maximum load in the load-slip curves. The value of k_{ser}, which denotes the secant slip modulus in the serviceability limit state of shear strength, was calculated using the following methodology Eq. (1):

$$k_{0.4} = \frac{0.4F_u}{\frac{4}{3}\left(s_{0.4} - s_{0.1}\right)} \tag{1}$$

Where F_{est} is the estimated ultimate shear capacity of the single-side specimens; F_u is half of F_{max}; $s_{0.1}$ indicates the slip at a load of 0.1Fu; $s_{0.4}$ indicates the slip at a load of 0.4Fu.

3 –FINITE ELEMENT INVESTIGATIONS

ABAQUS software [8] was used to perform three-dimensional numerical simulations for the push-out tests of timber-UHPC composite structures. Due to the double symmetry of the specimens, only a quarter of the push-out test arrangement was modelled. The analysis utilized the static general solution method. All components of the experimental analysis were represented, including UHPC slab, glulam beam, shear connectors, and reinforcement. The concrete damage plasticity (CDP) model was used to simulate the constitutive behavior of UHPC material. The sandhass model [9] was used to simulate the material properties of glulam. Both self-tapping screws and reinforcing steel were modelled using an ideal elastic-plastic constitutive model for finite element simulation. The contact between the screw and the UHPC notch, the screw and the glulam beam, and the UHPC slab and the glulam beam were modelled as surface-to-surface contact, with normal direction treated as hard contact and tangential direction simulated using coulomb friction. For the contact between the UHPC slab and the reinforcement steel, an embedded constraint was applied. The simulations accounted for the nonlinearities of the materials and the interactions between the system's components. A schematic diagram of the entire model is shown in Figure 5.

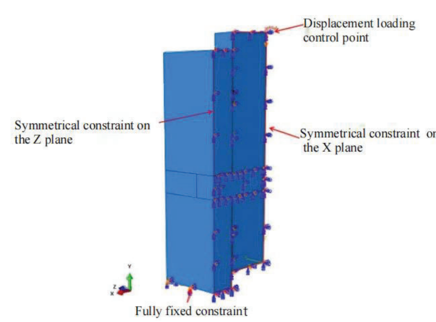

Figure 5. A sketch map of boundary condition and loading

4 – RESULTS

4.1 EXPERIMENTAL RESULTS

The load-slip curves are shown in Figure 6. The average shear capacity ranged from 120.84 to 285.11 kN, with corresponding average slip varying from 2.12 to 7.47 mm. The notch length and notch depth played an important role in the load-carrying capacity and slip stiffness of the specimens, which combined a notch and two screws.

The summary of tests results are shown in Table 4. When the notch depth increased from 20mm to 50mm, This increase in shear capacity and slip modulus, which were significant 64% and 42.3% when the notch depth was augmented from 20mm to 50mm, This is due to the change in the failure mode of the specimens from the ductile compressive failure of the glulam (at 20mm) to the brittle shear failure of the UHPC notch + screw (at 50mm). It can be seen that the bearing capacity of the notch + screw connection increases with the depth of the notch, which has a significant effect, but deeper notches are more likely to lead to brittle failure of the connection, thereby reducing its ductility. The load-slip curves of the notch depth is shown in Figure 6a). The shear length in front of the notch for the SA-70-50-200-2, SA-70-50-400-2, and SA-70-50-600-2 specimens were 200mm, 400mm, and 600mm, respectively. By comparing the ultimate bearing capacity and interface slip results of these three series of connections, it was observed that the ultimate bearing capacity increased slightly in a linear manner with the increase in shear length in front of the notch, with an increase of approximately 5.0%. It was worth noting that there was a significant difference in slip between the SA-70-50-200-2 and SA-70-50-400-2 specimens, which was due to the SA-70-50-200-2 specimens experiencing shear failure along the grain of the glulam, a brittle failure mode. The notch lengths for the SA-70-50-400-2, SA-110-50-400-2, and SA-150-50-400-2 specimens were 70mm, 110mm, and 150mm, respectively. By comparing the ultimate bearing capacity and interface slip results of these three series of connections, it was observed that when the notch length increased from 70mm to 150mm, the ultimate bearing capacity increased by approximately 48.9%, and the corresponding maximum slip increased by 48.1%. This indicated that both the bearing capacity and interface slip of the notch + screw connections increased with the depth of notch, showing a significant effect.

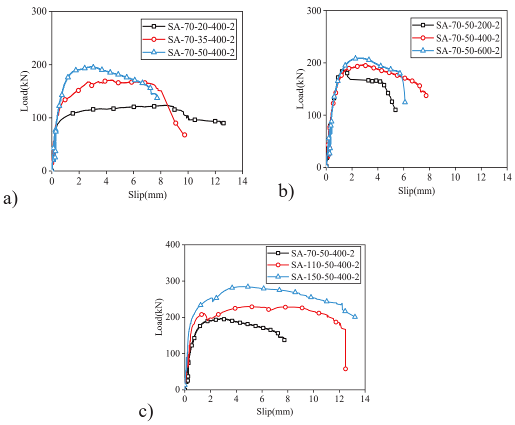

Figure 6. Load-slip curve: a)notch depth; b) shear length in front of the notch; c) notch length.

Table 4: Summary of test results.

Series	F_{max} (kN)	v_{max} (mm)	$K_{0.4}$ (kN/mm)
SA-70-20-400-2	241.68	7.47	219.54
SA-70-35-400-2	355.78	3.38	273.18
SA-70-50-400-2	396.22	2.49	312.30
SA-110-50-400-2	458.04	5.02	501.92
SA-150-50-400-2	570.22	4.80	691.35
SA-70-50-200-2	376.88	2.51	236.26
SA-70-50-600-2	419.04	2.43	3 15.24

The typical failure modes observed in the push-out tests are depicted in Figure 7. The main failure modes include four types: shear failure: shear failure of timber adjacent to the notch, parallel to the grain (TS); timber compression failure, either parallel or perpendicular to the grain (TC); shear-off failure of the UHPC at the interface between UHPC slabs and the glulam block (CS); shear failure of screws (SS).

Specimen SA-70-35-400-2 had glulam compression failure first, followed by UHPC shear failure (TS+TC), as shown in Figure 7a). Specimens SA-70-50-400-2 and SA-70-50-600-2 suffered the UHPC shear failure (CS), as shown in Figure 7b). Specimen SA-70-50-200-2 exhibited longitudinal timber shear failure along the notch bottom, attributed to a diminutive ratio between the timber length in front of the notch and the notch depth (TS), as evidenced in Figure 7c). Specimens SA-70-20-400-2、SA-110-50-400-2、SA-150-50-400-2 suffered a combination of glulam compression failure and glulam

https://doi.org/10.52202/080513-0137

shear failure (TC+TS), as shown in Figure 7d). All specimens exhibited the shear failure of screws (SS).

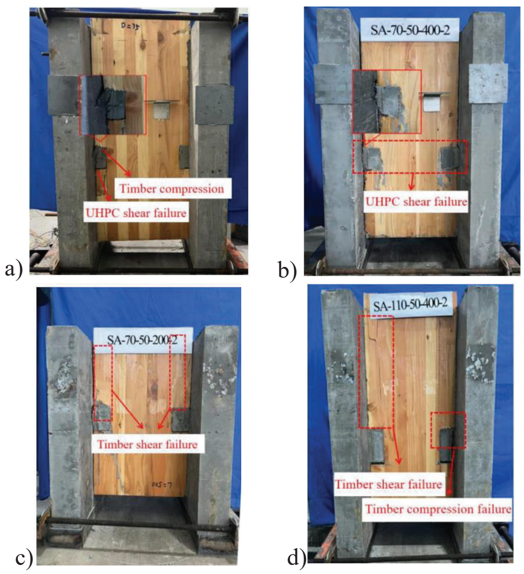

Figure 7. Typical failure modes: a) TS+TC+SS; b)CS+SS; c)TS+SS; (d)TC+TS+SS.

The variation trend of the slip stiffness of the connector with the shear length in front of the notch, notch depth and notch length are shown in Figure 8. By comparing the test results of the specimens SA-70-20-400-2, SA-70-35-400-2, and SA-70-50-400-2, it can be observed that the slip stiffness of the notch +screw connection increases with the depth of the notch. Specifically, when the notch depth increased from 20mm to 50mm, the slip stiffness ($k_{0.4}$) of the connection increases by approximately 42.3%.

By comparing the test results of the SA-70-50-200-2 and SA-70-50-400-2 specimens, as shown in Figure 8b), it was found that as the shear length in front of the notch increased, the slip stiffness of the connection also increased accordingly. The slip stiffness of the SA-70-50-400-2 and SA-70-50-600-2 specimens were almost identical, as both sets exhibit similar experimental phenomena and failure modes, with shear failure occurring only at the UHPC notch.

By comparing the test results of the SA-70-50-400-2, SA-110-50-400-2, and SA-150-50-400-2 specimens, as shown in Figure 8c), it was observed that the slip stiffness of the notch + screw connection increases with the length of the notch, which was consistent with the variations in ultimate bearing capacity and interface slip. Among these, the variation in slip stiffness near failure for the SA-150-50-400-2 specimens was similar to that of the SA-70-20-400-2 specimens. Specifically, when the connection was loaded to its yield or ultimate bearing capacity, the slip stiffness decreases rapidly, which was detrimental to the load-bearing behavior of the connection near the ultimate state.

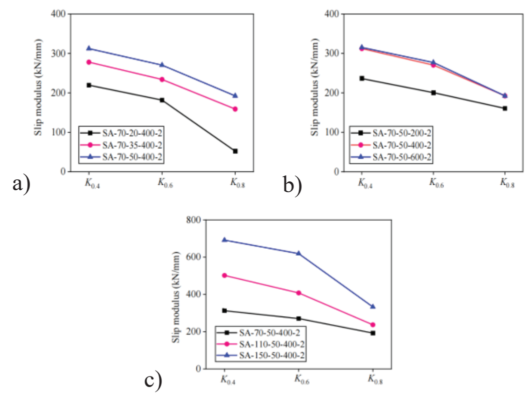

Figure 8. Comparison of slip stiffness of connectors: a) notch depth; b) Shear length in front of the notch; c) notch length.

4.2 NUMERICAL RESULTS

Figure 9 displays the comparison between the numerical and the experimental results, including failure modes and load-slip curves, where it can be observed a good correlation. A stress state analysis was conducted for specimens with typical failure modes. Stress cloud maps of the screws, UHPC slabs, and glulam beam components were selected from visualization processing, and compared with the actual failure modes of the connection components.

By comparing the experimental failure images and stress cloud maps of the specimens SA-150-50-400-2, it was found that for the specimens experiencing compression and shear failure in the glulam, the stress was mainly concentrated on the compression surface at the upper edge of the glulam notch, as shown in Figure 9a). At the time of failure, the compressive stress at the upper edge of the notch reached its maximum, reaching the compressive strength parallel to the grain of the glulam, 37.6 MPa.

By comparing the experimental failure images and stress cloud maps of the specimens SA-70-50-400-2, it was found that the failure mode obtained from the finite element simulation matched well with the experimental failure modes, as shown in Figure 9b). In the specimens where shear failure occurred at the UHPC notch + screw interface, damage gradually developed from top to bottom at the interface between the UHPC notch and the UHPC slabs. Meanwhile, shear forces were transferred from the UHPC notch to the screw, causing shear deformation of the screw at this interface. Ultimately, screw reached the limit stress state, with the UHPC notch being sheared and the screw being severed.

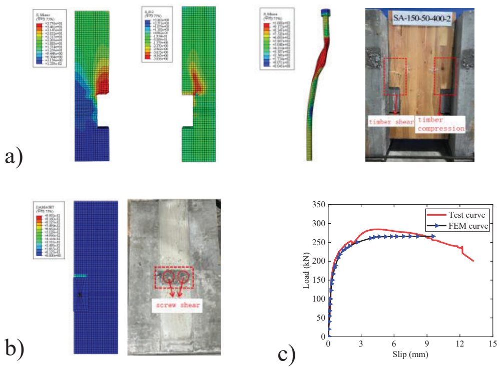

Figure 9: Comparison of numerical modeling and experimental results : (a) glulam+screw; (b)UHPC slab; c) load-slip curve.

5 – CONCLUSIONS

This paper presents a comprehensive study of notch+screw connectors with in GUCC structures, employing both experimental and analytical methods. Based on the presented results, the following conclusions can be drawn:

1. Typical failure modes of the notch+screw connectors included the compression failure of glulam, the shear failure of glulam, and the shear failure of UHPC notch, where the compression failure of glulam exhibits ductile behavior while the other two exhibit brittle behavior.
2. Experimental observations indicate that shallow notches tend to fail in a ductile manner but exhibit lower stiffness and strength. In contrast, deeper notches enhance both stiffness and shear capacity, though they are more susceptible to brittle failure.
3. The shear capacity and slip stiffness of the notch+screw connectors increased proportionally with the increase in notch depth and notch length. The shear length in front of the notch had an insignificant effect on the shear capacity and initial stiffness.
4. Comparing the finite element calculation results with experimental results, the accuracy of the finite element simulation method used in this study was validated.

ACKNOWLEDGEMENTS

The authors express their sincere gratitude for the financial support provided by the National Key R&D Program of China (2021YFF0501004); the National Natural Science Foundation of China (No. 52478135); Chongqing Natural Science Foundation (Grant No. CSTB2024NSCQMSX0572); Open Research Fund for Key Laboratory of Building Structure Reinforcement and Underground Space Engineering, Ministry of Education (Grant No. MEKL202204); the Entrepreneurship and Innovation Support Program for Overseas-educated student in Chongqing China (Grant No. CX2021085).

REFERENCES

[1] Dias, Alfredo. Design of timber-concrete composite structures: A state-of-the-art report by COST Action FP1402/WG 4. Shaker Verlag, 2018.

[2] Zhang, Lei, et al. Experimental investigation on the structural performance of mass timber panel-concrete composite floors with notched connections. Journal of Structural Engineering 148.2 (2022): 04021249.

[3] BS EN 13183-1:2002. Moisture content of a piece of a sawn timber-Part 1: determination by oven dry method: BSI, British Standards Institution, 2002.

[4] EN 408. Timber structure-Structural timber and glued laminated timber -Determination of some physical and mechanical properties, European Committee for Standardization, Brussels, Belgium, 2009.

[5] ASTM International. D 905-08 Standard Test Method for Strength Properties of Adhesive Bonds in Shear by Compression Loading; ASTM International: West Conshohocken, PA, USA, 2013.

[6] T CBMF 37-201. Fundamental characteristics and test methods of ultra-high performance concrete, China Building Material Council, Beijing, China, 2018.

[7] EN 26891. Timber structure-Joint made with mechanical fastener-General principles for the determination of strength and deformation characteristic, European Committee for Standardization, Brussels, Belgium, 1991.

[8] ABAQUS. Software Documentation. Version 6.14 by Simulia; 2014.

[9] Sandhaas C, Van de Kuilen J W G. Mechanical behaviour of timber joints with slotted-in steel plates[J]. Civil Engineering & Geosciences. 2012.

https://doi.org/10.52202/080513-0137